Available online at www.sciencedirect.com

SCIENCE DIRECT

European Journal of Pharmacology 508 (2005) 23–30

www.elsevier.com/locate/ejphar

Characterization of voltage-dependent gating of $P2X_2$ receptor/channel

Ken Nakazawa[a,*], Yasuo Ohno[b]

[a]Cellular and Molecular Pharmacology Section, Division of Pharmacology, National Institute of Health Sciences, 1-18-1 Kamiyoga, Setagaya, Tokyo 158-8501, Japan

[b]Division of Pharmacology, National Institute of Health Sciences, 1-18-1 Kamiyoga, Setagaya, Tokyo 158-8501, Japan

Received 9 September 2004; received in revised form 29 November 2004; accepted 6 December 2004
Available online 4 January 2005

Abstract

The role of a voltage-dependent gate of recombinant $P2X_2$ receptor/channel was investigated in *Xenopus* oocytes. When a voltage step to −110 mV was applied from a holding potential of −50 mV, a gradual increase was observed in current evoked by 30 μM ATP. Contribution of this voltage-dependent component to total ATP-evoked current was greater when the current was evoked by lower concentrations of ATP. The voltage-dependent gate closed upon depolarization, and half the gates were closed at −80 mV. On the other hand, a potential at which half the gates opened was about −30 mV or more positive, which was determined using a series of hyperpolarization steps. The results of the present study suggest that the voltage-dependent gate behavior of $P2X_2$ receptor is not due to simple activation and deactivation of a single gate, but rather due to transition from a low to a high ATP affinity state.

Keywords: P2X receptor; Voltage dependence; Gate; Kinetics; Ligand affinity

1. Introduction

Extracellular ATP is considered a neurotransmitter, and its fast neurotransmission is mediated through ion channel-forming P2X receptors (see reviews, Ralevic and Burnstock, 1998; Khakh, 2001; North, 2002). To date, at least seven subclasses of P2X receptor ($P2X_{1-7}$) have been cloned, which form homo- or heteromeric receptors that act as functional ion channels (North and Surprenant, 2000). Each subclass consists of two transmembrane domains (TM1 and TM2) and one long extracellular domain (E1) between them. Both TM1 (Jiang et al., 2001; Haines et al., 2001) and TM2 (Rassendren et al., 1997; Egan et al., 1998; Migita et al., 2001) contribute to formation of the channel pore. P2X receptor/channels are permeable to cations, but demonstrate poor cation selectivity. The channels are gated by ATP molecules, and the narrowest part of the channel pore opens when activated (Rassendren et al., 1997). The ATP-binding site for gating is partly attributable to basic amino acid residues near the outer mouth of the channel pore formed by TM1 and TM2 (Ennion et al., 2000; Jiang et al., 2000), and the possibility that aromatic residues in E1 contribute to the binding site has also been suggested (Nakazawa et al., 2002; Roberts and Evans, 2004).

In addition to ATP, other factors are known to modulate channel activity. Zn^{2+} and acidic conditions facilitate ATP-mediated gating by increasing ATP sensitivity of $P2X_2$ receptor (Clyne et al., 2002). Neurotransmitters, including dopamine, and related compounds also facilitate ATP-mediated gating (Nakazawa et al., 1997a). Membrane potential may also play a role. It has been reported that ionic current activated by ATP is enhanced by hyperpolarization in pheochromocytoma PC12 cells (Nakazawa et al., 1997b). We observed similar voltage-dependent gating of recombinant $P2X_2$ receptor/channel, which was originally cloned from PC12 cells (Brake et al., 1994), and qualitatively analyzed its properties in the present study.

2. Methods

Recordings of ionic current through recombinant $P2X_2$ receptor/channels were performed according to our previous

* Corresponding author. Tel.: +81 3 3700 9704; fax: +81 3 3707 6950.
E-mail address: nakazawa@nihs.go.jp (K. Nakazawa).

0014-2999/$ - see front matter © 2004 Elsevier B.V. All rights reserved.
doi:10.1016/j.ejphar.2004.12.005

report (Nakazawa and Ohno, 1997). Briefly, the cloned rat $P2X_2$ receptor (Brake et al., 1994) was expressed in *Xenopus* oocytes by injecting in vitro transcribed cRNA. After 4 days of incubation at 18 °C, the membrane current of the oocytes was recorded. Oocytes were bathed in ND96 solution containing (in mM) NaCl 96, KCl 2, $CaCl_2$ 1.8, $MgCl_2$ 1, HEPES 5 (pH 7.5 with NaOH). In some experiments, oocytes were bathed in solution containing 10.8 mM $BaCl_2$ instead of 1.8 mM $CaCl_2$. When achieving a low extracellular chloride concentration, 96 mM Na-acetate was added instead of 96 mM NaCl. ATP (adenosine 5′ -triphosphate disodium salt; Sigma, St. Louis, MO, U.S.A.) was applied by superfusion for approximately 10 s at regular 2-min intervals. Membrane current was recorded using the standard two-electrode voltage-clamp techniques, and electrical signals were stored on a data recorder (PC204Ax; SONY, Tokyo, Japan) for off-line analysis. Curve fittings to data were made using Microsoft' Excel X.

3. Results

3.1. Voltage-dependent component of ATP-evoked current

Fig. 1A compares membrane currents in the absence and presence of 30 μM ATP in a $P2X_2$ receptor-expressing oocyte. The oocyte was held at −50 mV and stepped to −110 mV for 200 ms. In the presence of ATP, inward current at −110 mV did not instantaneously reach steady-state, but gradually increased: a biphasic increase in current was observed with a voltage-independent component ("a" in Fig. 1A) and a voltage-dependent component ("b" in Fig. 1A). When the voltage was returned to −50 mV, a gradually declining inward "tail" current was observed ("c" in Fig. 1A). The voltage-dependent component of the inward current at −110 mV was observed to follow first-order kinetics with a time constant of 40 ms (Fig. 1B).

Fig. 2A demonstrates an increased magnitude of the voltage-dependent component when activated from a less negative holding potential. The voltage-dependent component was larger when the step to −110 mV was applied from −10 mV ("a" in Fig. 2A) than when it was applied from −70 mV ("b" in Fig. 2A). This dependence of the voltage-dependent component on holding potentials is illustrated in Fig. 2B. It is worth noting that Ca^{2+}-activated currents exist in *Xenopus* oocytes (Weber, 1999; Zhang and Hamill, 2000). Since P2X receptor/channels are Ca^{2+}-permeable (Khakh, 2001), a secondarily activated Ca^{2+}-induced current might contribute to the observed voltage-dependent changes. This does not, however, appear to be the case since a similar dependence on holding potentials was observed when extracellular Ca^{2+} was replaced with 10.8 mM Ba^{2+}. Time constants for the activation of the voltage-dependent component were obtained as shown in Fig. 1B, and the mean values were plotted against holding potentials

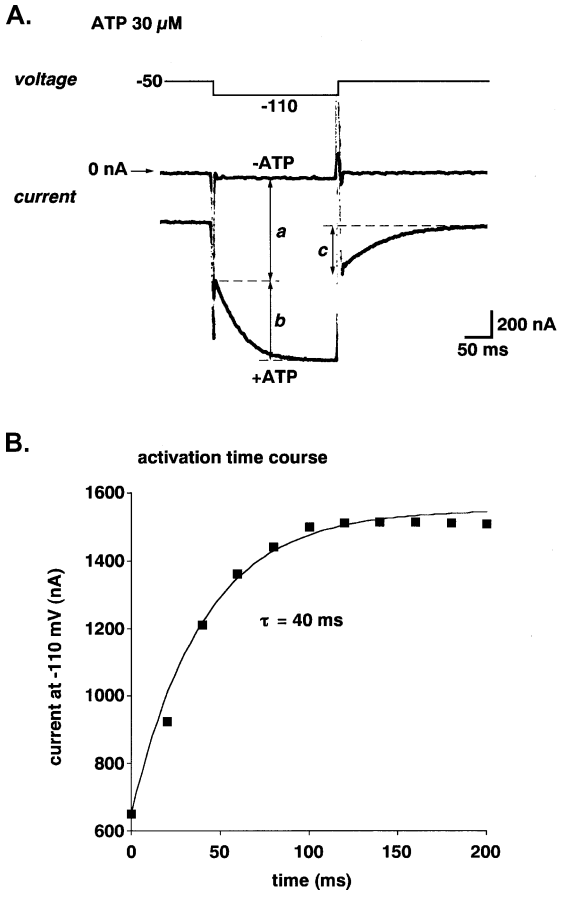

Fig. 1. (A) Current traces of an oocyte stepped to −110 mV from a holding potential of −50 mV in the absence (−ATP) or presence (+ATP) of 30 μM ATP. The current evoked by ATP is represented by the difference between the two traces. Upon hyperpolarization, a gradual increase in current was observed in the presence of ATP, suggesting activation of a voltage-dependent gate (denoted by "b"). The current denoted by "c" represents a gradually declining "tail current" that was observed when the voltage was returned to −50 mV. (B) Time course of activation of the voltage-dependent component. Current amplitude of the voltage-dependent component represented by "b" in panel A was plotted against time after the onset of hyperpolarization at −110 mV. The voltage-dependent component could be made to fit a curve with a time constant of 40 ms.

(Fig. 2C). While the current amplitude demonstrated voltage dependence (Fig. 2B), voltage did not have an effect on time course of the activation.

3.2. Effect of ATP concentrations

Fig. 3A shows the voltage-dependent component of the current activated by 10 μM or 300 μM of ATP in a single oocyte. The relative size of the voltage-dependent component involved in total ATP-evoked current became smaller when the current was evoked by greater concentrations of ATP (Fig. 3A and B). A similar dependence on ATP concentration was observed for the current evoked in the presence of 10.8 mM Ba^{2+} instead of 1.8 mM Ca^{2+} (Fig. 3B). Dependence on ATP concentrations was also found for activation time constants for the voltage-

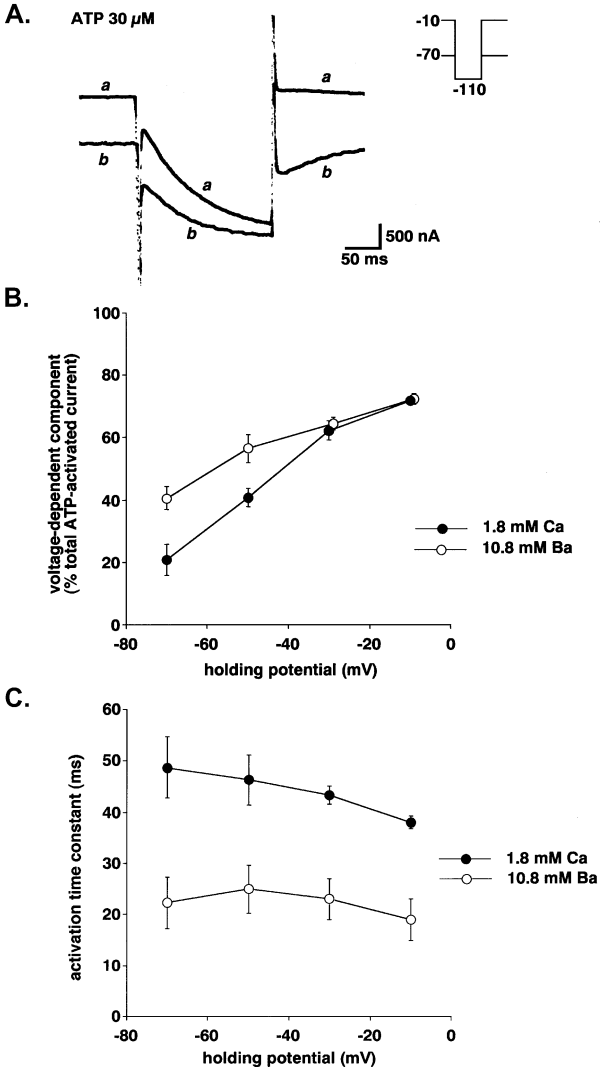

Fig. 2. Effect of holding potential on current. Current was evoked by 30 μM ATP. (A) Voltage-dependent current at −110 mV when stepped from a holding potential of −10 mV ("a") or −70 mV ("b"). (B) Effect of holding potential on voltage-dependent current. The amplitude of the voltage-dependent current was measured as described in Fig. 1A. Mean values obtained from 4 oocytes in a standard extracellular solution containing 1.8 mM Ca^{2+} (●) and an extracellular solution containing 10.8 mM Ba^{2+} (instead of Ca^{2+}; ○) were plotted. Bars represent the S.E.M. (C) Time course of activation of the voltage-dependent component. Time constants were determined as shown in Fig. 1B, and mean values obtained from 4 oocytes were plotted against holding potentials. Bars represent the S.E.M.

dependent component; the time constants were larger for 10 μM ATP than 30 μM ATP (Fig. 3C).

3.3. Activation and deactivation kinetics

Cl^- currents are observed in *Xenopus* oocytes (Weber, 1999; Zhang and Hamill, 2000). In the following experiments, current measurements were made using an extracellular solution containing 96 mM Na-aspartate instead of NaCl in order to facilitate the analysis of the voltage-dependent component of ATP-evoked current by reducing Cl^- currents. In doing so, there was an obvious reduction in outward current upon depolarization, resulting in better voltage-clamp conditions. Using this extracellular solution, the EC_{50} value for ATP-activated current measured at −50 mV was about 40 μM, which was lower than the value obtained with the standard extracellular solution containing 96 mM NaCl (about 100 μM; Nakazawa and Ohno, 2004). Fig. 4 illustrates

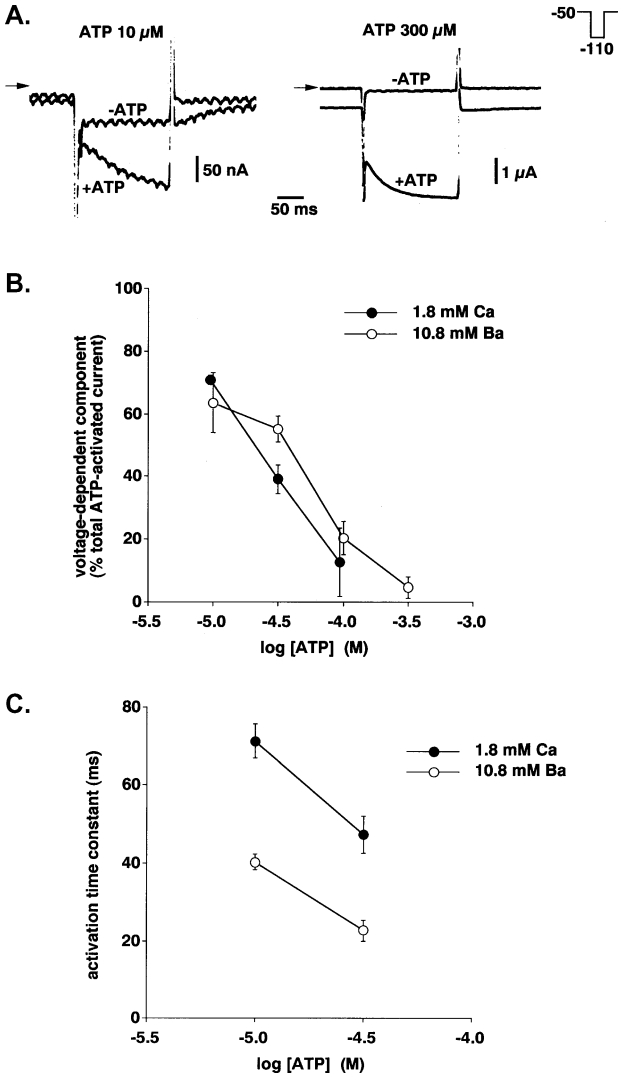

Fig. 3. Effect of ATP concentration. The voltage-dependent current was activated by hyperpolarization (−110 mV) from a holding potential of −50 mV. (A) Voltage-dependent current activated by 10 μM or 30 μM ATP. Current traces in the absence (−ATP) or presence (+ATP) of ATP are superimposed in each panel. (B) Contribution of the voltage-dependent current to total ATP-evoked current using different ATP concentrations. Mean values obtained from 4 oocytes in a standard extracellular solution containing 1.8 mM Ca^{2+} (●) and an extracelllular solution containing 10.8 mM Ba^{2+} (instead of Ca^{2+}; ○) were plotted. Bars represent the S.E.M. (C) Time course of activation of the voltage-dependent components. Time constants were determined as shown in Fig. 1B, and mean values obtained from 4 oocytes were plotted against holding potentials. Bars represent the S.E.M.

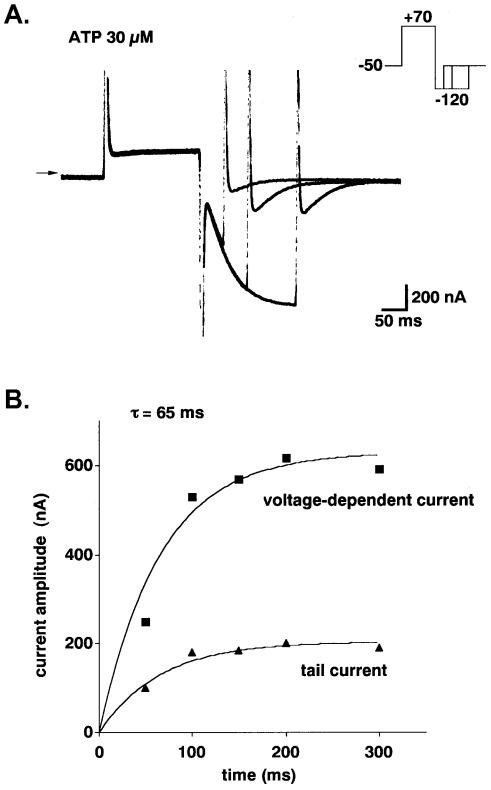

Fig. 4. Activation and tail current. (A) Gradual increase in magnitude of the tail current with increasing voltage-dependent current. Current traces obtained upon exposure to hyperpolarizing pulses (−120 mV) of different durations are superimposed. (B) Time course of activation of the voltage-dependent (■) and tail (▲) currents. Current amplitude was plotted against duration of hyperpolarization (also shown in panel A). The results of both time course activation experiments fit curves with a single time constant of 65 ms.

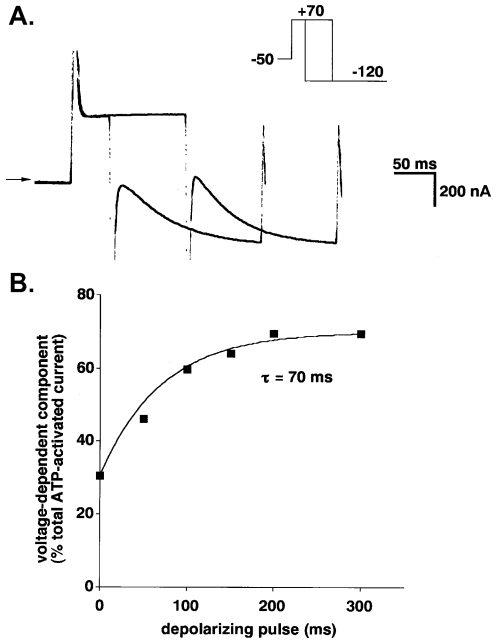

Fig. 5. Deactivation of the voltage-dependent component. (A) Current traces obtained using depolarizing pulses (+70 mV) of two different durations. The amplitude of the voltage-dependent component increased when the duration was prolonged. (B) Time course of deactivation of the voltage-dependent component. Current amplitude was plotted against duration of the depolarizing pulses (also shown in panel A).

the relation between activation kinetics of the voltage-dependent component and time course of tail current. As shown in Fig. 4A, oocytes were stepped to 70 mV and then to −120 mV to induce the voltage-dependent component. When hyperpolarization at −120 mV was terminated after various periods, a gradual increase in amplitude of the tail current was observed with increased duration of hyperpolarization at −120 mV. Time courses of both the voltage-dependent component and tail current could be fitted with curves with a single time constant (65 ms in this case; Fig. 4B). Similar fitting with single time constants were made for 4 oocytes tested, and the mean time constant±S.E.M. was 66.3±2.4 ms.

With increased duration of the +70 mV depolarizing pulse, increased amplitude of the voltage-dependent component was observed at −120 mV (Fig. 5A). This may reflect "deactivation" of the voltage-dependent component (Scheme 1):, where A is ATP, and R and R* are closed and open states, respectively, of the voltage-dependent component of $P2X_2$ receptor/channel. The deactivation time course could be fitted with a time constant of 70 ms in this case (Fig. 5B; mean±S.E.M., 71.3±1.3 ms; n=4).

3.4. Voltage dependence of activation and deactivation

As shown in Fig. 1, contribution of the voltage-dependent component to total ATP-evoked current was influenced by the holding potential prior to hyperpolarization. This was further examined by testing a number of prepulses at various potentials prior to hyperpolarization (Fig. 6A). As the prepulse became more depolarized, a greater contribution of the voltage-dependent component to total ATP-evoked current was observed, and this contribution became maximal near 0 mV (Fig. 6B). Thus, the voltage-dependent gate must be completely closed at potentials equal to or more positive than 0 mV. The data were fitted with a curve in accordance with the following model of "deactivation":

$$d_\infty = 1/\{1 + \exp[(E_{1/2} - E_m)/k]\}, \quad (1)$$

where d_∞ represents the relative proportion of closed gates at steady state, $E_{1/2}$ is the voltage at which the half-maximal closing occurs, E_m is the membrane potential, and

$$AR \underset{\text{(deactivation)}}{\overset{\text{(activation)}}{\rightleftharpoons}} AR^*$$

Scheme 1.

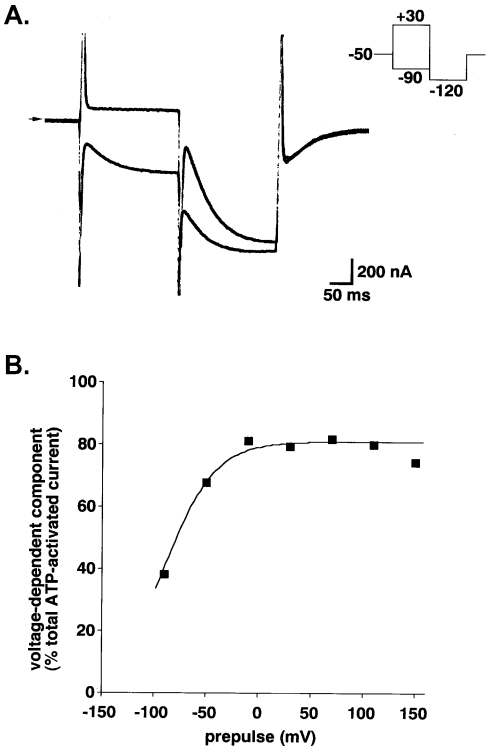

Fig. 6. Prepulse experiment. An ATP concentration of 30 μM was used. (A) Current traces obtained using prepulses of +30 mV ("a") or −90 mV ("b") prior to hyperpolarization at −120 mV. (B) Effect of prepulses. The relative contribution of the voltage-dependent current to total ATP-evoked current at −120 mV was plotted against each prepulse voltage. Some of this data is also shown in panel A.

k is a slope factor reflecting an energy barrier (Hodgkin and Huxley, 1952; Hille, 1992a). As shown in Fig. 6B, potential at which half the gates closed was estimated to be −90 mV in this case (mean±S.E.M., −78.8±5.2 mV; n=4).

The voltage dependence of activation was also examined. As shown in Fig. 7A, the channels responsible for the voltage-dependent component was sufficiently "deactivated" by applying a prepulse of +100 mV, and they were then activated at various hyperpolarization potentials. Contribution of the voltage-dependent component to total ATP-evoked current decreased as the hyperpolarization became more negative up to −45 mV in the case shown in Fig. 7B. Potentials exceeding −45 mV could not be examined since the resultant ATP-evoked current was not large enough to analyze. The data were fitted in accordance with the following model of "activation":

$$a_\infty = 1/\{1+\exp[(E_{1/2}-E_m)/k]\}, \quad (2)$$

where a_∞ represents the degree of gate opening at steady state. The other parameters are the same as those described above. The data obtained using Eq. (2) (Fig. 7B) could be fitted with a curve indicating that half of the gates were open at a potential of −30 mV.

The above data suggest that activation of the voltage-dependent gate occurs at more positive potentials than gate deactivation. To further investigate this, the fraction of the gates that escaped deactivation ($1-d_\infty$) was calculated from the data obtained during deactivation experiments. The deactivation data was then plotted alongside data obtained from activation experiments (Fig. 7C). These data suggest that the activation potential is 50 mV more positive than the deactivation potential.

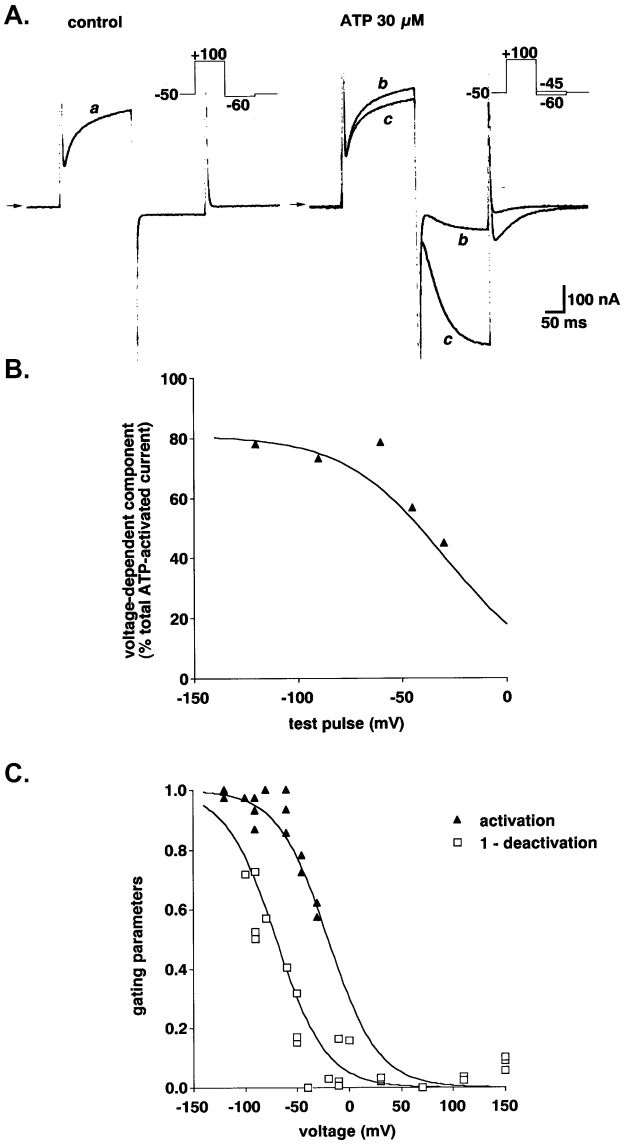

Fig. 7. Effect of hyperpolarization on voltage-dependent current. (A) Current traces before (control) and during the application of 30 μM ATP. In the panel on the right, two current traces obtained following hyperpolarization at −45 mV ("b") and −60 mV ("c") are superimposed. (B) Contribution of voltage-dependent current to total ATP-evoked current at various hyperpolarization potentials. Some of these data are shown in panel A. (C) Comparison of activation and deactivation. Parameters describing activation and deactivation were determined as described in the text. Each data point represents data obtained from individual oocytes.

4. Discussion

4.1. Schematic model of voltage-dependent gating

Recombinant $P2X_2$ receptor/channels expressed in *Xenopus* oocytes exhibited voltage-dependent gating properties similar to those of the channels in PC12 cells (Nakazawa et al., 1997b). The following similarities were observed: (1) the gate opens at negative potentials, (2) activation follows a time course with a time constant of 40 to 70 ms, and (3) gating depends on ATP concentrations. Thus, voltage-dependent gating in PC12 cells may be due to intrinsic expression of $P2X_2$ receptor/channels. We depict here a model that has been proposed to explain voltage-dependent gating of the channels in PC12 cells (Scheme 2):, where A is ATP, R_L and R_H represent closed states, and R* represents the open state (Nakazawa et al., 1997b). In this model, voltage-dependent gating is explained by transition between low and high ATP-affinity states. Upon hyperpolarization, there is a shift from the R_L to the R_H conformation. ATP preferentially binds to channels in the R_H state ($A \cdot R_H$), after which the channels open ($A \cdot R_H$*). Binding of ATP is the rate-limiting step since activation kinetics were observed to depend on ATP concentrations in the present study (Fig. 3C). The following rate constants have been proposed (Scheme 3): where k_{+1} parallels the concentration of ATP ($k_{+1}=k'_{+1}$[ATP]), and K_d is given by k_{-1}/k'_{+1} (Hille, 1992b). In the present experiment, an activation time constant of 65 ms was observed in the presence of 30 μM of ATP (Fig. 4), which is equivalent to a rate constant of 15 s^{-1}. Using these values, $k'_{+1}=k_{+1}/[ATP]=15\ s^{-1}/(30\ \mu M)=5\times10^5\ M^{-1}\ s^{-1}$. An inactivation time constant of 70 ms was observed in the presence of 30 μM of ATP (Fig. 5), which is equivalent to a rate constant of 14 s^{-1}. Thus, K_d was calculated to be $k_{-1}/k'_{-1}=14\ s^{-1}/(5\times10^5\ M^{-1}\ s^{-1})=28\ \mu M$, which is slightly less than the EC_{50} value obtained at −50 mV (about 40 μM). This estimation is in accordance with the finding that the voltage-dependent component is not completely activated at −50 mV (Fig. 7C). It is difficult to quantify the low-affinity ATP binding state since the relationship between concentration and response needs to be assessed at highly positive potentials, while $P2X_2$ receptor/channels permit only small current due to their inward-rectifying nature. We estimate here the low affinity from simple theoretical concentration–response curves. Fig. 8 shows two concentration–response curves. One demonstrates an EC_{50} of 30 μM, corresponding to a high-affinity state. If the other low-affinity state demonstrates an EC_{50} of 100 μM, more $P2X_2$ receptor/channels were in the high-affinity state in the presence of 10 μM ATP, and more were in the low-affinity state in the presence of 300 μM ATP. This is consistent with the greater observed contribution of the voltage-dependent component to total ATP-evoked current in the presence of 10 μM, while little was observed in the presence of 300 μM ATP (Fig. 3). Thus, the low-affinity state may be lower than the high-affinity state by threefold or larger.

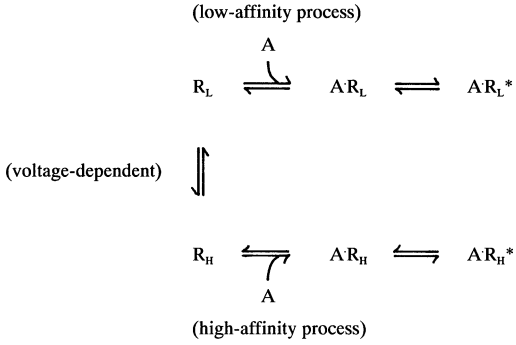

Scheme 2.

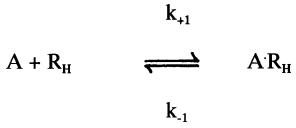

Scheme 3.

The idea of the transition of $P2X_2$ receptor/channels between low- and high-affinity states might explain the "non-voltage-dependent" component of ATP-evoked current. For example, the current evoked by 30 μM ATP was not completely observed as voltage-dependent component even when activated at very negative potentials (Fig. 7B) or following deactivation at very positive potentials (Fig. 6B). This "non-voltage-dependent current" (about 20% of the total ATP-evoked current) might result from the activation of $P2X_2$ receptor/channels in the low-affinity state prior to voltage-dependent activation.

The voltage dependence of activation and deactivation differed, with deactivation occurring at more negative potentials (Fig. 7C). This indicates that the activation and the deactivation do not arise from a simple reversible "back-and-forth" process, rather, two voltage-dependent processes

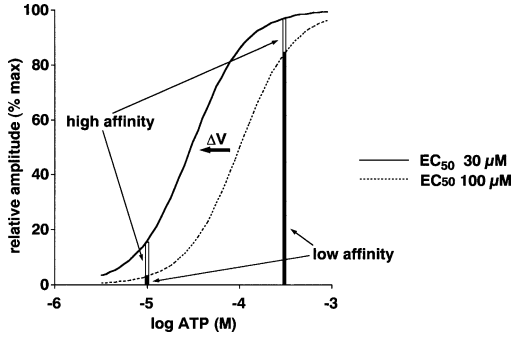

Fig. 8. Voltage-dependent change in sensitivity to ATP might explain dependence of the voltage-dependent current on ATP concentration. Low-affinity (EC_{50}=100 μM) and high-affinity (EC_{50}=30 μM) states of the receptor are thought to exist (Hill coefficient; 1.5). Each receptor shifts from a low-affinity to a high-affinity state upon hyperpolarization (ΔV). With 10 μM ATP, only a small proportion of the receptors, many of which were in the low-affinity state, were activated prior to hyperpolarization, but many more were activated upon induction of the high-affinity state by hyperpolarization. In the presence of 300 μM ATP, a larger proportion of the receptors were activated even in the low-affinity state, and induction of the high-affinity state caused only a marginal increase in activated receptors.

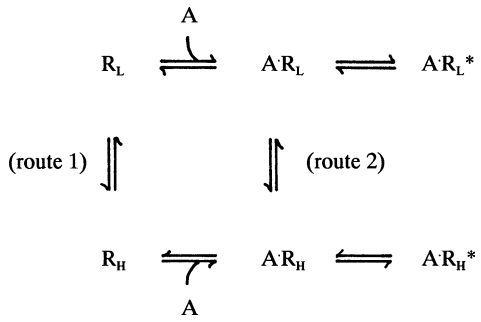

Scheme 4.

may be involved. We propose the following modification to Scheme 2.

This model (Scheme 4) involves two voltage-dependent processes, one resulting in activation through "route 1", and the other resulting in deactivation through "route 2". Such model would explain the observed difference in voltage dependence between activation and deactivation. However, we would expect this model to result in more difficult to interpret data than we did above based on Schemes 2 and 3.

4.2. Relevance of voltage-dependent gating

$P2X_2$ receptor is expressed in a number of neurons (e.g., Atkinson et al., 2000; Rubio and Soto, 2001). $P2X_2$ receptor/channel is permeable to Ca^{2+} (Egan and Khakh, 2004), and Ca^{2+} influx through the channel may influence cellular activity, although its exact role remains to be clarified. The voltage-dependent gating reported here may be relevant to the Ca^{2+} influx from the following consideration. Na^+ current (I_{Na}) and Ca^{2+} current (I_{Ca}) permeating through $P2X_2$ receptor/channel are:

$$I_{Na} = -P_{Na}\frac{E_m F^2}{RT}\frac{[Na]_o}{1-\exp(-EF/RT)} \quad (3)$$

$$I_{Ca} = -4P_{Ca}\frac{E_m F^2}{RT}\frac{[Ca]_o \exp(-2EF/RT)}{1-\exp(-2EF/RT)}, \quad (4)$$

where P_{Na} and P_{Ca} represent the permeability of Na^+ and Ca^{2+}, respectively, E_m represents the membrane potential, and F, R, and T are their usual physicochemical meanings (Fatt and Ginsborg, 1958; Nakazawa et al., 1989). The ratio of I_{Na} to I_{Ca} is thus:

$$\frac{I_{Ca}}{I_{Na}} = \frac{4P_{Ca}[Ca]_o}{P_{Na}[Na]_o}\frac{1}{\exp(E_m F/RT)[\exp(E_m F/RT)+1]} \quad (5)$$

This equation indicates that the ratio of I_{Ca}/I_{Na} is larger at more negative potentials. The ratio calculated at −90 mV is about 13-fold larger than that calculated at −30 mV. Thus, channel opening at negative potentials favors Ca^{2+} over Na^+ influx. Thus, voltage-dependent gating may facilitate cellular Ca^{2+}-dependent responses when cells are hyperpolarized. This may occur when efflux through K^+ channels outpaces depolarization afforded by opening of $P2X_2$ receptor/channels.

4.3. Conclusion

The results of the present study suggested that $P2X_2$ receptor exhibits voltage-dependent gating, and that this is not due to simple activation and deactivation of a single gate, but rather, due to a transition from a low ATP affinity to a high ATP affinity state. This may favor Ca^{2+} influx at negative potentials, although further studies are required to clarify the physiological significance of voltage-dependent gating of $P2X_2$ receptor.

Acknowledgements

This work was supported, in part, by a Health and Labour Science Research Grant for Research on Advanced Medical Technology from the Ministry of Health, Labour and Welfare, Japan, as well as a grant-in-aid for scientific research from the Ministry of Education, Science, Sports and Culture, Japan (KAKENHI 13672319) awarded to K.N.

References

Atkinson, L., Batten, T.F., Deuchars, J., 2000. $P2X_2$ receptor immunoreactivity in the dorsal vagal complex and area postrema of the rat. Neuroscience 99, 683–696.

Brake, A.J., Wagenbach, M.J., Julius, D., 1994. New structural motif for ligand-gated ion channels defined by an ionotropic ATP receptor. Nature 371, 519–523.

Clyne, J.D., LaPointe, L.D., Hume, R.I., 2002. The role of histidine residues in modulation of the rat $P2X_2$ purinoceptor by zinc and pH. J. Physiol. 539, 347–359.

Egan, T., Khakh, B.S., 2004. Contribution of calcium ions to P2X channel responses. J. Neurosci. 24, 3413–3420.

Egan, T.M., Haines, W.R., Voigt, M.M., 1998. A domain contributing to the ion channel of ATP-gated $P2X_2$ receptors identified by the substituted cysteine accessibility method. J. Neurosci. 18, 2350–2359.

Ennion, S., Hagan, S., Evans, R.J., 2000. The role of positively charged amino acids in ATP recognition by human $P2X_1$ receptors. J. Biol. Chem. 275, 29361–29367.

Fatt, P., Ginsborg, B.L., 1958. The ionic requirements for the production of action potentials in crustacean muscle fibres. J. Physiol. 142, 516–543.

Haines, W.R., Migita, K., Cox, J.A., Egan, T.M., Voigt, M.M., 2001. The first transmembrane domain of the P2X receptor subunit participates in the agonist-induced gating of the channel. J. Biol. Chem. 276, 32793–32798.

Hille, B., 1992a. Classical biophysics of the squid giant axon. Ionic channels of excitable membranes, Second Edition. Sinauer, Sunderland, MA, pp. 23–58.

Hille, B., 1992b. Ligand-gated channels of fast chemical synapses. Ionic channels of excitable membranes, Second Edition. Sinauer, Sunderland, MA, pp. 140–169.

Hodgkin, A.L., Huxley, A.F., 1952. The dual effect of membrane potential on sodium conductance in the giant axon of *Loligo*. J. Physiol. 116, 497–506.

Jiang, L.H., Rassendren, F., Surprenant, A., North, R.A., 2000. Identification of amino acid residues contributing to the ATP-binding site of a purinergic P2X receptor. J. Biol. Chem. 275, 34190–34196.

Jiang, L.H., Rassendren, F., Spelta, V., Surprenant, A., North, R.A., 2001. Amino acid residues involved in gating identified in the first membrane-spanning domain of the rat $P2X_2$ receptor. J. Biol. Chem. 276, 14902–14908.

Khakh, B.S., 2001. Molecular physiology of P2X receptors and ATP signalling at synapses. Nat. Rev. 2, 165–174.

Migita, K., Haines, W.R., Voigt, M.M., Egan, T.M., 2001. Polar residues of the second transmembrane domain influence cation permeability of the ATP-gated $P2X_2$ receptor. J. Biol. Chem. 276, 30934–30941.

Nakazawa, K., Ohno, Y., 1997. Effects of neuroamines and divalent cations on cloned and mutated ATP-gated channels. Eur. J. Pharmacol. 325, 101–108.

Nakazawa, K., Fujimori, K., Takanaka, A., Inoue, K., 1989. An ATP-activated conductance in pheochromocytoma cells and its suppression by extracellular calcium. J. Physiol. 428, 257–272.

Nakazawa, K., Liu, M., Inoue, K., Ohno, Y., 1997a. pH dependence of facilitation by neurotransmitters and divalent cations of $P2X_2$ purinoceptor/channels. Eur. J. Pharmacol. 337, 309–314.

Nakazawa, K., Liu, M., Inoue, K., Ohno, Y., 1997b. Voltage-dependent gating of ATP-activated channels in PC12 cells. J. Neurophysiol. 78, 884–890.

Nakazawa, K., Ojima, H., Ohno, Y., 2002. A highly conserved tryptophane residue indispensable for cloned rat neuronal P2X receptor activation. Neurosci. Lett. 324, 141–144.

North, R.A., 2002. Molecular physiology of P2X receptors. Physiol. Rev. 82, 1013–1067.

North, R.A., Surprenant, A., 2000. Pharmacology of cloned P2X receptors. Annu. Rev. Pharmacol. Toxicol. 40, 563–580.

Ralevic, V., Burnstock, G., 1998. Receptors for purines and pyrimidines. Pharmacol. Rev. 50, 413–492.

Rassendren, F., Buell, G., Newbolt, A., North, R.A., Surprenant, A., 1997. Identification of amino acid residues contributing to the pore of a P2X receptor. EMBO J. 16, 3446–3454.

Roberts, J.A., Evans, R.J., 2004. ATP binding at human $P2X_1$ receptors. Contribution of aromatic and basic amino acids revealed using mutagenesis and partial agonists. J. Biol. Chem. 279, 9043–9055.

Rubio, M., Soto, F., 2001. Distinct localization of P2X receptors at excitatory postsynaptic specializations. J. Neurosci. 21, 641–653.

Weber, W.-M., 1999. Ion currents of *Xenopus laevis* oocytes: state of the art. Biochim. Biophys. Acta 1421, 213–233.

Zhang, Y., Hamill, O.P., 2000. Calcium, voltage- and osmotic stress sensitive currents in *Xenopus* oocytes and their relationship to single mechanically gated channels. J. Physiol. 523, 83–99.